Least-squares finite element methods for the Navier-Stokes equations for generalized Newtonian fluids

Serdar Serdas[1*], **Alexander Schwarz**[1], **Jörg Schröder**[1], **Stefan Turek**[2], **Abderrahim Ouazzi**[2], and **Masoud Nickaeen**[2]

[1] Institute of Mechanics, Faculty of Engineering, University of Duisburg-Essen, Universitätsstr. 15, 45117 Essen, Germany
[2] Institute for Applied Mathematics, Faculty of Mathematics, TU Dortmund University, Vogelpothsweg 87, 44227 Dortmund, Germany

In this contribution we present the least-squares finite element method (LSFEM) for the incompressible Navier-Stokes equations. In detail, we consider a non-Newtonian fluid flow, which is described by a power-law model, see [1]. The second-order problem is reformulated by introducing a first-order div-grad system consisting of the equilibrium condition, the incompressibility condition and the constitutive equation, which are written in residual forms, see [2]. Here, higher-order finite elements which are an important aspect regarding accuracy for the present formulation are investigated.

1 Introduction

The classical LSFEMs provide some theoretical and computational advantages, see e.g. [3], but there are still difficulties concerning, e. g. the mass conservation, especially when lower-order interpolants are used, see [4]. Besides the application of some weighting factors, a possible solution is the consideration of higher interpolations, see e.g. [5]. In the present work, we compare quadratic and cubic formulations for non-Newtonian fluids by a numerical example.

2 Least-squares method

We consider the velocity-stress-pressure approach for the stationary non-Newtonian fluid equations which are given by the balance of momentum, mass conservation and the material equation as following

$$\rho \nabla \boldsymbol{v}\, \boldsymbol{v} - \operatorname{div} \boldsymbol{\sigma} = \mathbf{f}, \qquad \operatorname{div} \boldsymbol{v} = 0 \qquad \text{and} \qquad \boldsymbol{\sigma} - 2\rho\, \nu(D_{II}) \nabla^s \boldsymbol{v} + p\mathbf{I} = \mathbf{0} \tag{1}$$

with some suitable boundary conditions. Here, $\boldsymbol{\sigma}$ denotes the Cauchy stresses, $\mathbf{f}$ the forcing function, $\boldsymbol{v}$ the velocities, p the pressure, ρ the density, and $\nu(\cdot)$ is the (nonlinear) viscosity. The symmetric part of the deformation rate tensor is defined as $\nabla^s \boldsymbol{v} = \frac{1}{2}\left(\nabla \boldsymbol{v} + [\nabla \boldsymbol{v}]^T\right)$ and the second invariant of the deformation rate tensor as $D_{II} = \frac{1}{2}(2\nabla^s \boldsymbol{v} \cdot 2\nabla^s \boldsymbol{v})$. Here, we chose for the viscosity function the power-law model to describe the non-Newtonian fluid behavior

$$\nu(D_{II}) \quad = \quad \nu_0\, D_{II}^{\frac{n-1}{2}}, \qquad (\nu_0 > 0) \tag{2}$$

where ν_0 is the zero shear rate viscosity and n the flow behavior index which distinguishes between different type of fluids. For $n = 1$, we recover the Newtonian fluid (constant viscosity). For $n > 1$ one obtain shear-thickening (or dilatant) fluids (viscosity increases with increase in shear-rate) and for $n < 1$ shear-thinning (or pseudoplastic) fluids (viscosity decreases with increase in shear-rate). Furthermore, we replace the nonlinearities such as the convective term and viscosity term by the Newton linearization technique. Using quadratic L^2-norms, the linearized physically weighted least-squares functional is constructed as

$$\begin{aligned} \mathcal{J}_{lin}(\boldsymbol{v}, \boldsymbol{\sigma}, p; \boldsymbol{v}^k) \quad &= \quad \frac{1}{2}\, || \frac{1}{\sqrt{\rho}} (\rho \nabla \boldsymbol{v}^k\, \boldsymbol{v} + \rho \nabla \boldsymbol{v}\, \boldsymbol{v}^k - \operatorname{div} \boldsymbol{\sigma} - \mathbf{f}) + \mathcal{Q}^k_{conv} ||^2_0 + \frac{1}{2}\, ||\operatorname{div} \boldsymbol{v}||^2_0 \\ &+ \quad \frac{1}{2}\, || \frac{1}{\sqrt{\rho \nu(D_{II})^k}} (\boldsymbol{\sigma} - 2\,\rho\, \nu(D_{II})^k \nabla^s \boldsymbol{v} - 8\,\rho\, \nu'(D_{II})^k (\nabla^s \boldsymbol{v} \cdot \nabla^s \boldsymbol{v}^k) \nabla^s \boldsymbol{v}^k + p\mathbf{I}) + \mathcal{Q}^k_{vis} ||^2_0. \end{aligned} \tag{3}$$

where the index k is taken as either an initial guess or as a known quantity from the immediate previous iteration. $\mathcal{Q}^k_{conv}$ and $\mathcal{Q}^k_{vis}$ are denoting terms from the linearization which are only related to known values. The minimization of $\mathcal{J}_{lin}$ requires the first variation $\delta \mathcal{J}_{lin}$ to be equal to zero. We use mixed finite elements $RT_m P_k P_l$, where P_k and P_l denote Lagrange shape functions of polynomial order k for the velocities and l for the pressure. RT_m denotes Raviart-Thomas interpolants of polynomial order m for a conforming discretization of the stresses. Further remarks regarding the minimization of $\mathcal{J}_{lin}$ or the used finite element spaces are given in [3] and [6].

* Serdar Serdas: Email serdar.serdas@uni-due.de, phone: +00 49 201 183-3792, fax: +00 49 201 183-2680

3 Numerical example

As a numerical example we solve a fully developed power law fluid flow between parallel plates. Figure 1 shows the flow domain and the boundary conditions. Due to the symmetry, we consider only the upper half of the domain.

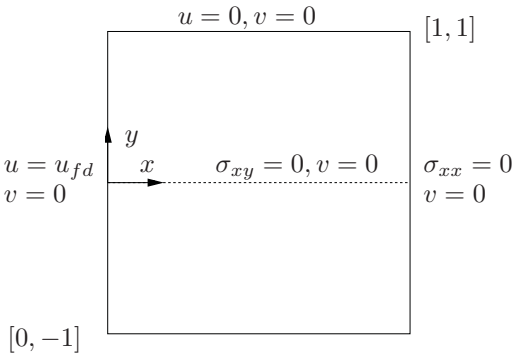

Fig. 1: Boundary value problem for a fully developed power law fluid flow between parallel plates.

For the inflow boundary condition, the horizontal velocity $u_{fd} = \frac{u}{u_{avg}}$ is imposed by the analytical velocity profile (4) and the vertical velocity is set equal to zero. The upper edge has no-slip boundary conditions, the symmetry line a zero shear-stress σ_{xy} and zero vertical velocity $v = 0$. The outflow has a zero normal-stress boundary condition $\sigma_{xx} = 0$ and a zero vertical velocity $v = 0$. The material parameter such as the density ρ and the flow consistency ν_0, are set to one.

$$u_{fd} = \frac{2n+1}{n+1}(1 - y^{\frac{n+1}{n}}), \qquad y = [0, 1] \tag{4}$$

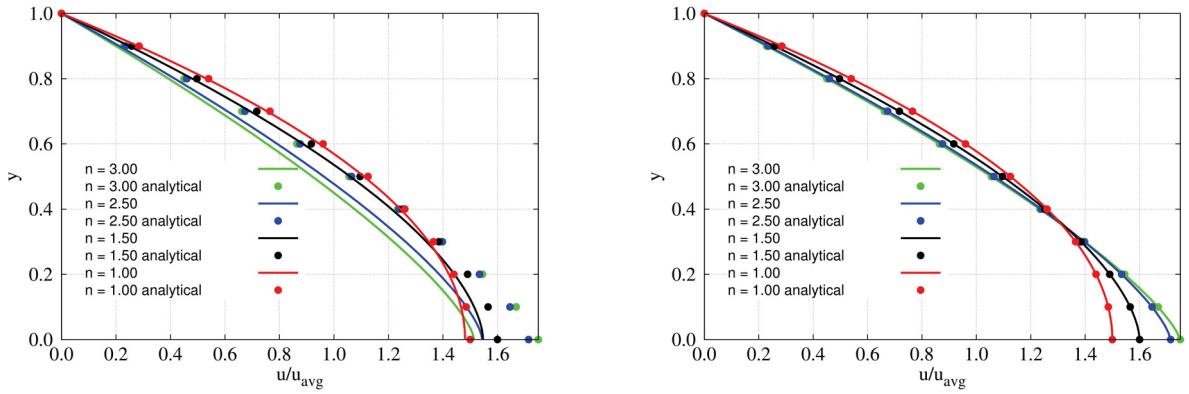

Fig. 2: Comparison of the velocity profiles with the analytical solution for various power law index values regarding shear-thickening fluids for $RT_0P_2P_1$ (left) and $RT_1P_3P_1$ (right) discretizations.

Figure 2 depicts various flow behavior index for shear-thickening fluids. On the left, the results for the $RT_0P_2P_1$ (62,339 dofs) and on the right the $RT_1P_3P_1$ (40,643 dofs) discretizations can be seen. The results of the outflow velocities are compared with the analytical velocity profile (4). As could be expected, an increase of the parameter n in (2) leads to a more steeper velocity profile. Considering the $RT_0P_2P_1$ discretization, it turns out that the lower-order discretization shows difficulties to predict the analytical solutions whereas the higher-order discretization matches very well with the analytical solution.

Acknowledgements MERCUR Pr-2011-0017: “Effiziente Simulationstechniken für robuste Least-Squares FEM in der Fluiddynamik”

References

[1] B.C. Bell, and K.S. Surana, IJNMF **18**, 127–162 (1994).
[2] P.B. Bochev and M.D. Gunzburger, CMAME **126**, 267–287 (1995).
[3] B.N. Jiang, The Least-Squares Finite Element Method. Springer-Verlag, (1998).
[4] S. Serdas, A. Schwarz, J. Schröder, S. Turek, A. Ouazzi and M. Nickaeen, PAMM **13**, 301–302 (2013).
[5] M. Nickaeen, A. Ouazzi and S. Turek, JOCP **256**, 416–427 (2014).
[6] A. Schwarz and J. Schröder, PAMM **11**, 589–590 (2011).